A method for increasing the supersolvus critical strain for recrystallization in single-crystal superalloys

Lin, Sicong; Chen, Kai; Zeng, Qiang; Ramamurty, Upadrasta

2023

Lin, S., Chen, K., Zeng, Q. & Ramamurty, U. (2023). A method for increasing the supersolvus critical strain for recrystallization in single-crystal superalloys. Materials Research Letters, 11(10), 856-862. https://dx.doi.org/10.1080/21663831.2023.2253267

https://hdl.handle.net/10356/171571

https://doi.org/10.1080/21663831.2023.2253267

Materials Research Letters

ISSN: (Print) (Online) Journal homepage: https://www.tandfonline.com/loi/tmrl20

A method for increasing the supersolvus critical strain for recrystallization in single-crystal superalloys

Sicong Lin, Kai Chen, Qiang Zeng & Upadrasta Ramamurty

To cite this article: Sicong Lin, Kai Chen, Qiang Zeng & Upadrasta Ramamurty (2023) A method for increasing the supersolvus critical strain for recrystallization in single-crystal superalloys, Materials Research Letters, 11:10, 856-862, DOI: 10.1080/21663831.2023.2253267

To link to this article: https://doi.org/10.1080/21663831.2023.2253267

MATER. RES. LETT.
2023, VOL. 11, NO. 10, 856–862
https://doi.org/10.1080/21663831.2023.2253267

MATERIALS RESEARCH LETTERS
Taylor & Francis
Taylor & Francis Group

ORIGINAL REPORTS
OPEN ACCESS
Check for updates

A method for increasing the supersolvus critical strain for recrystallization in single-crystal superalloys

Sicong Lin[a], Kai Chen[a], Qiang Zeng[b] and Upadrasta Ramamurty[c,d]

[a]Center for Advancing Materials Performance from the Nanoscale (CAMP-Nano), State Key Laboratory for Mechanical Behavior of Materials, Xi'an Jiaotong University, Xi'an, People's Republic of China; [b]Beijing Key Laboratory of Advanced High Temperature Materials, Central Iron and Steel Research Institute, Beijing, People's Republic of China; [c]School of Mechanical and Aerospace Engineering, Nanyang Technological University, Singapore, Singapore; [d]Institute of Materials Research Engineering, Agency for Science, Technology and Research, Singapore, Singapore

ABSTRACT

Recrystallization, possibly triggered during heat treatments by plastic strains of only 1–2%, is highly deleterious to Ni-based single-crystal superalloys. Herein, we successfully recover plastic deformation and enhance the supersolvus critical strain for recrystallization by ramping the annealing temperature slowly from 1100 °C to γ'-solvus point. This preempts recrystallization during the subsequent supersolvus solutionizing treatment. The proposed method is validated in single-crystals compressed to 5.9% plastic strain at room temperature. After supersolvus solutionizing, an almost dislocation-free single-crystal with uniformly distributed γ'-precipitates is obtained. The proposed method offers a practical means to bring down the overall expenses of single-crystal turbine blades.

ARTICLE HISTORY
Received 24 July 2023

KEYWORDS
Recovery heat treatment; Ni-based superalloy single crystals; recrystallization critical strain; microstructure evolution

IMPACT STATEMENT

An optimized pre-solutionizing recovery heat treatment can elevate the critical plastic strain value for recrystallization in Ni-based superalloy single-crystals to 3 times higher than previously established.

1. Introduction

Ni-based single crystal (NBSC) superalloys have been widely used for high-pressure turbine engine blades with complex geometries in modern aeronautical and energy-generation industries [1]. Plastic deformation and associated microscopic defects such as dislocations are likely to be introduced into them in almost every stage of their production: from manufacture to assembly to transportation [2]. Then, either during the mandated post-manufacturing heat treatment or during high-temperature service, those dislocations can trigger recrystallization (RX), which results in a polycrystalline microstructure with high-angle grain boundaries (HAGBs) [3–6]. Since HAGBs can severely degrade the high-temperature creep and fatigue resistances of the NBSC parts [7], every effort is made to optimize the heat treatment protocols such that any dislocation introduced during the plastic deformation are either eliminated or minimized. In the process, the excess stored energy is relieved, and thus RX is prevented [2,8,9].

Typically, a supersolvus solutionizing step during the heat treatment is necessary for imparting chemical and microstructural homogeneity that, in turn, will lead to an optimized mechanical performance of the superalloy. RX can occur easily during this step. To measure the recovery capability of a given NBSC, its supersolvus critical plastic strain, $\epsilon*$, is identified. It is defined to as the plastic strain, ϵ_p, above which RX cannot be preempted during the supersolvus solutionizing treatment.

It is apparent that a higher $\epsilon*$ leads to a lower rejection rate of the NBSC part during the quality control exercise. It, in turn, would result in lowering of the

CONTACT Kai Chen kchenlbl@gmail.com Center for Advancing Materials Performance from the Nanoscale (CAMP-Nano), State Key Laboratory for Mechanical Behavior of Materials, Xi'an Jiaotong University, Xi'an, Shaanxi 710049, People's Republic of China

Supplemental data for this article can be accessed here. https://doi.org/10.1080/21663831.2023.2253267

overall expenses associated with the manufacturing and maintenance of the NBSC superalloy blades. Although $\epsilon*$ depends on the deformation temperature, even the highest value of it reported hitherto for room temperature uniaxial compressive deformation is only between 1% and 2% [2,10]. Successful recovery annealing at 1100 °C for 6 h has been reported recently to preempt recrystallization in the 3D-printed NBSC superalloys which intrinsically contain high and nonuniformly distributed residual strains [11]. However, it remains unclear whether such protocol is also effective to those with externally imposed strains, and whether and how the protocol can be optimized to enhance $\epsilon*$.

In this paper, we propose and validate a novel heat treatment protocol that involves a sub-solvus recovery annealing by slowly ramping the temperature, to lower the stored energy first and hence minimize the driving force for RX, prior to standard supersolvus solutionizing. The validity of the new strategy is verified on an AM3 NBSC superalloy that was plastically deformed in uniaxial compression to a ϵ_p as high as 5.9%. Microstructural evolution during the recovery annealing was characterized in detail to understand the dislocation density reduction mechanisms. The proposed methodology provides a practical means to prevent the NBSC parts from recrystallizing into a polycrystalline microstructure, and thus enhance the finish product rate and lower the overall cost.

2. Material and methods

Cylindrical specimens with 5 mm diameter and 10 mm length were cut from solutionized [001] cast AM3 NBSC boules, a first-generation superalloy with the chemical composition of 7.9Cr, 5.5Co, 2.2Mo, 5.0W, 2.0Ti, 5.9Al, 3.6Ta, 0.002C, and balance Ni, all in weight percent. They were subjected to uniaxial compression to ϵ_p of 3.7%, 4.2%, 5.3 and 5.9% at a nominal strain rate of about $8 \times 10^{-5}\ s^{-1}$ at room temperature. ϵ_p in each specimen was measured from the relative reduction in length due to compression. The deformed cylinders were axially sectioned into two or four pieces for the recovery studies. As shown in Figure S1 in the Supplementary Information (SI), the dissolution of the γ'-precipitates starts at 1100 °C and gets completed at 1280 °C. On this basis, three types of recovery annealing protocols were selected (Figure S2 in SI). In Type 1, the recovery annealing temperature, T_R, was set constant at either 1100 or 1150 °C. In Type 2, T_R was increased in a stepwise manner, from 1100 to 1270 °C, which is 10 °C below the solvus temperature. In Type 3, T_R was ramped up continuously from 1100 °C to the γ' solvus temperature (1280 °C). The total time allowed for recovery in all these three heating methods was maintained approximately the same (∼2 h). After recovery annealing, each specimen was solutionized at 1300 °C (same to the standard solutionizing temperature of AM3) for 30 min, which was long enough for recrystallized grains, if any, to grow up to tens of microns or larger, which will enable their easy detection. For comparison, an identical specimen compressed to $\epsilon_p = 3.7\%$ was also solutionized without any recovery treatment. All the heat treatment experiments were carried out in a muffle furnace under air atmosphere. This led to the oxidization of the samples' surfaces. Therefore, the oxide layers were removed by mechanical peeling and polishing, before mounting the heat-treated specimens onto the 70° sample stage for the EBSD scans. The peeling and polishing led to the inevitable formation of rough edges and irregular corners on the sample cross-sections.

3. Results

Electron backscatter diffraction (EBSD) with a step size of 10 µm was used to map the crystal orientation of the specimens after the solutionizing treatment. Without recovery annealing, recrystallization occurs readily in the reference specimen subjected to a ϵ_p of 3.7%. In it, more than 20% of the scanned area is occupied by the recrystallized grains (Figure 1a). In contrast, a two-hour recovery at 1150 °C preempted recrystallization completely in the specimen with a ϵ_p of 4.2% (Figure 1b). Recovery was found to be highly sensitive to T_R. As demonstrated in Figure S3a of SI, annealing at 1100 °C for even 11 h does not result in sufficient recovery and hence cannot prevent recrystallization even in a specimen with $\epsilon_p = 3.7\%$. Thus, a higher T_R is necessary to recover the stored energy more thoroughly. Too high a T_R, however, can trigger recrystallization, as displayed in Figure S3b, when the temperature is ramped directly to the solvus temperature. To overcome this dilemma, Type 2 recovery, which involves multiple steps of annealing at incremental temperatures, is applied to a specimen with $\epsilon_p = 5.3\%$; Figure 1c shows that recrystallization is successfully prevented in it. When ϵ_p is increased further to 5.9%, HAGBs with misorientation angles of up to 30° are observed (Figure 1d). The continuous gradual ramp-up of Type 3 recovery strategy allows for an even higher finishing temperature without increasing the risk of recrystallization, and thus the supersolvus critical strain could be increased to 5.9% (Figure 1e). Although a 15° misorientation still exists over a millimeter-length scale after supersolvus solutionizing, no HAGBs could be detected. This confirms complete suppression of recrystallization. The misorientation present is not large enough to influence on high-temperature creep properties on NBSC superalloys in a significant manner [12,13]. Thus, the proposed protocol not only maintains the single-crystal

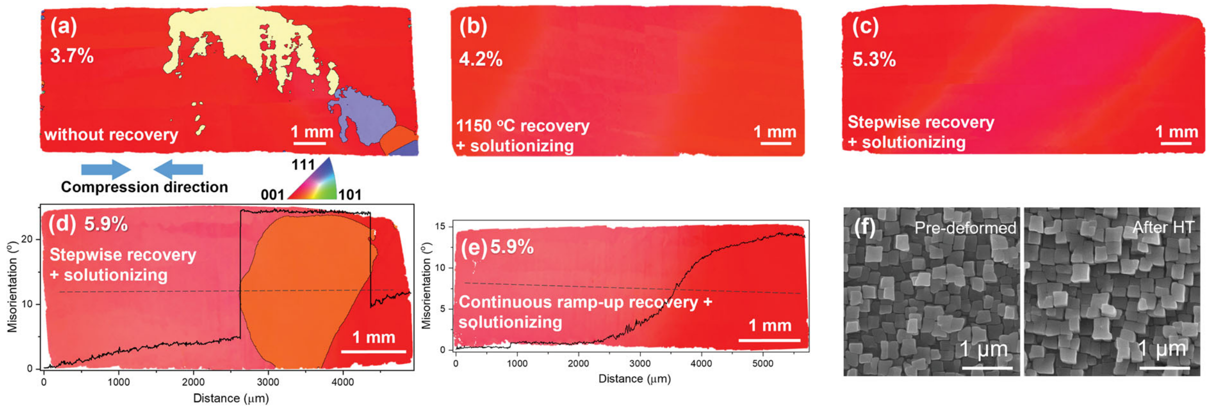

Figure 1. (a) to (e) Inverse pole figure (IPF) maps along the compression direction of the EBSD scanned cross-sections of specimens with various strain levels after recovery annealing and solutionizing treatment. (f) γ' morphologies before deformation and after heat treatment.

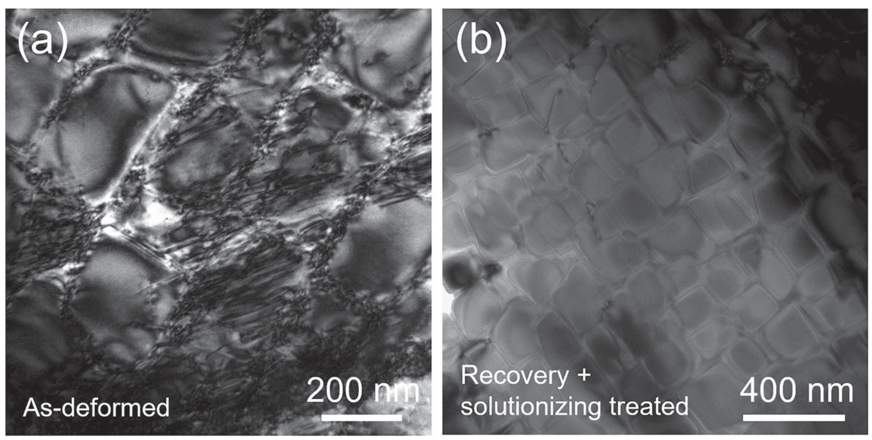

Figure 2. TEM observation of the dislocations in the 5.9% strained NBSC superalloy (a) before and (b) after recovery and subsequent solutionizing heat treatment.

structure, but also preserves the morphology and volume fraction of the γ'-precipitates (Figure 1f), fulfilling the requirements of a successful heat treatment.

Besides crystal orientation, the dislocation structures in the as-deformed and post-annealed superalloys are characterized using a transmission electron microscope (TEM). Prior to any heat treatment, a high density, ρ ($>5\times10^{14}$ m^{-2}, measured by using the line-intercept method [14]), of dislocations are observed in the narrow γ-channels in the sample with a ϵ_p of 5.9% (Figure 2a). In stark contrast, ρ is only 1×10^{13} m^{-2} (Figure 2b), i.e. less than one-fiftieth of that in the as-deformed state, after solutionizing treatment that incorporates the pre-solution recovery annealing.

To understand how the sub-solvus annealing assisted the plastic strain recovery, the microstructural evolution in the specimen with $\epsilon_p = 5.9\%$ is studied in detail. When the temperature is first increased rapidly to 1100 °C (the starting point of the continuous ramp-up recovery), the low magnification scanning electron microscope (SEM) image recorded under the secondary electron mode (Figure 3a) shows a grid-like structure at hundred-micron scale, with bright rectangular-shaped interiors and ~ 10 μm wide dark edges. A higher magnification image indicates that the dark and bright contrasts come from different γ' morphologies (Figure 3b). Dark edges consist coarsened γ'-particles. The coarsening directions in even an individual dark band are non-uniform, suggesting inhomogeneous strain distribution in the as-deformed sample (Figure 3c) [15]. In the relatively brighter rectangular regions, the γ'-particles retain their typical cuboidal shape, although some of them also show the tendency of coarsening, as highlighted with the yellow circles in Figure 3d. TEM characterization reveals the formation of dislocation networks at the γ/γ' interphase boundaries, while the γ'-particles are still dislocation-free (Figure 3e). Recovery annealing results in the partial dissolution of the primary γ'. As the specimen is cooled down, fine (~ 25 nm in diameter) secondary γ'-particles reprecipitate in the γ-channels. In

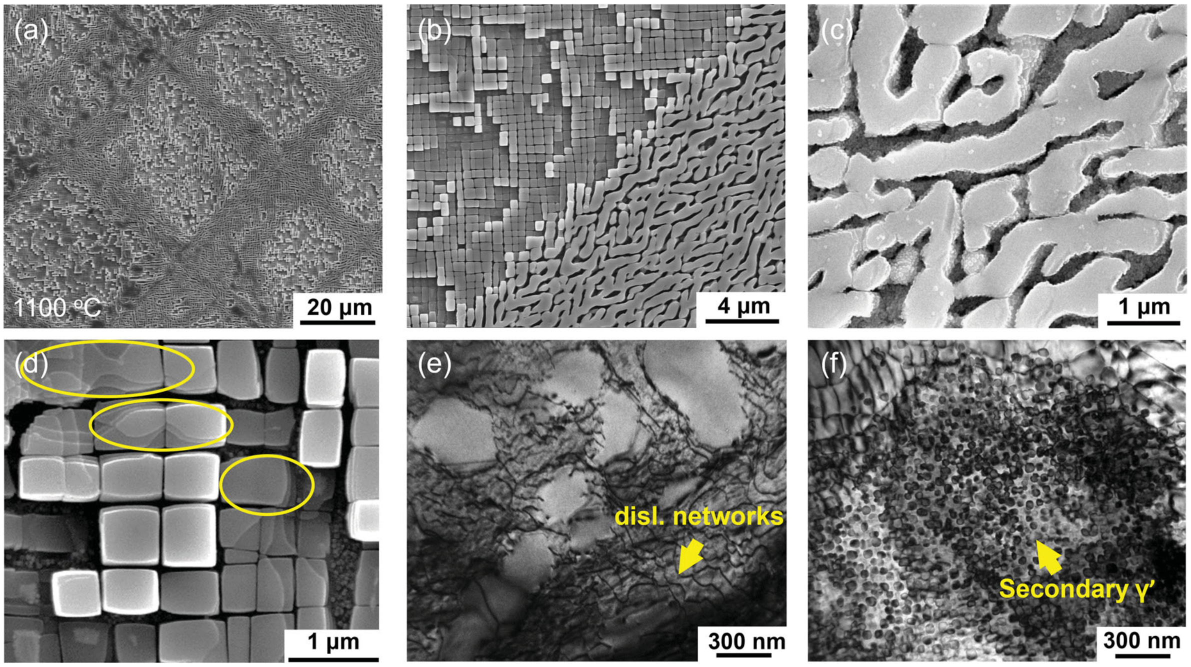

Figure 3. SEM and TEM characterizations of the specimen that was deformed and then subjected to recovery annealing at 1100 °C. Grid-like structures observed at (a) low and (b) high magnification in SEM. Morphologies of the (c) coarsened and (d) cuboidal γ' in the dark and bright contrast regions of (a), respectively. TEM image of the (e) coarsened γ' surrounded by dislocation networks at the γ'/γ interphase while the (f) secondary γ' rich regions are almost dislocation-free.

secondary γ' dominated regions, almost no dislocations are found (Figure 3f).

As the temperature is ramped slowly to 1150 °C (Figure 4a), the grid-like structure is replaced by the widely distributed coarsened γ'-precipitates across the whole sample. More secondary γ'-particles (with an average size of 50 nm) are observed in the widened γ-channels that are present between the coarsened primary γ'-particles. Similar to the case in Figure 3f, dislocation networks are only observed at the γ/γ' interphase boundaries. When the temperature is further elevated to 1270 °C, differences in the microstructures of dendritic core and interdendritic regions are noted. These are a result of the micro-segregation induced solvi variation between these two regions (Figure S1) [16]. This differentiates the overall microstructure from that annealed at relatively low temperatures (compare Figure 3 and Figure 4a, for example). In the dendrite cores, full solutionization is accomplished (Figure 4b), and thus a uniform cuboidal-shaped γ' microstructure is obtained; all the dislocations have been fully annihilated. In the interdendritic regions, however, γ' is not fully solutionized (evidenced by the high-volume fraction of fine secondary γ'-particles and coarsened primary ones in the SEM image), and thus some dislocations remain at the interphase boundaries between the undissolved primary γ'-precipitates and the γ-matrix (Figure 4c).

4. Discussion

On the basis of the observed microstructural evolution, the mechanisms of plastic deformation and its recovery during annealing are discussed below. Most of the dislocations induced by the room-temperature plastic deformation (for up to $\sim$6% plastic strains) occur within the narrow γ-channels. Considering that the volume fraction of the γ-matrix is only $\sim$30%, forcing such a high density of dislocations within it is energetically unfavorable. During the pre-solutionizing recovery annealing, 'pipe' diffusion, which is facilitated by the pre-existing dislocations, takes place easily near the localized deformation regions [17,18]. Thus, both partial dissolution and coarsening of the γ'-particles are accelerated at elevated temperatures, resulting in mobile γ/γ' interphase boundaries. Consequently, the dislocations, whose mobility was resisted or even pinned by the γ'-precipitates, become mobile again. The broadened γ channels provide sufficient space for them to interact with each other. In the process, dislocation annihilation and formation of networks, both of which result in the lowering of the stored energy, are promoted. Further increase in T_R leads to a reduction in the volume fraction of γ'-particles and the decomposition of the dislocation networks that form at the γ/γ' interphase boundaries. These mechanisms, in turn, further bring down the stored energy, and thus preempt

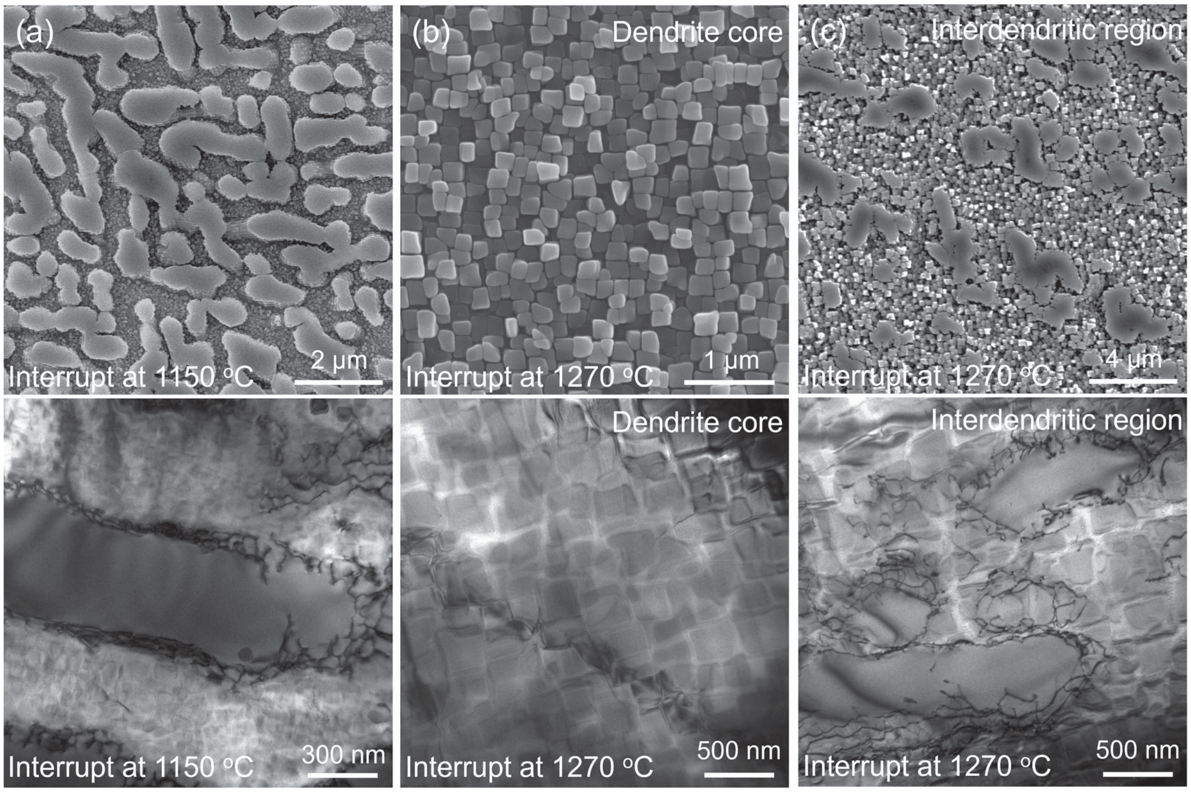

Figure 4. Microstructure of the specimen that was deformed to a plastic strain of 5.9% and then recovery annealed at high-temperature. (a) SEM and TEM characterization showing the evidence the coarsening of γ'-particles and formation of dislocation networks after annealing at 1150 °C. As the temperature is slowly ramped to 1270 °C, (b) dendrite cores are composed of uniform γ'-particles and almost no dislocations, while (c) low volume fraction of primary γ'-particles and low density of dislocations are observed in the interdendritic zones.

RX from occurring even when the temperature is further increased above the solvus point. In the absence of a proper recovery protocol, in contrast, recrystallization will be triggered during supersolvus annealing in a short period of time. As demonstrated through Figure S4, dislocation slip bands are observed in the as-deformed specimen. Within these bands, although misorientations of $\sim 4^{\mathrm{o}}$ is accumulated gradually over a length scale of about 400 μm, the pixel-to-pixel orientation change is on the order of only 0.6$^{\mathrm{o}}$ or less. However, after only 3 min annealing at 1300 °C, recrystallized grains and high-angle grain boundaries are rendered in the deformed specimen, probably due to the rapid migration of the polygonization-induced boundaries and the interaction between such boundaries and the dislocations within its swept area. This illustrates the necessity of recovery heat treatment in preventing recrystallization. The partially dissolved γ'-particles not only release the dislocations from the γ/γ' interface, create more spaces for dislocations to annihilate and rearrange into low-energy configurations, but also constrain the long-range motion of dislocations to form high-angle grain boundaries.

The experimental observations establish that higher annealing temperatures favor a complete recovery of the stored energy. On the other hand, if directly annealed at high-temperatures, the deformed NBSC superalloys may undergo recrystallization; the rendered HAGBs will then migrate quickly to ruin the single-crystal microstructure. Thus, the protocol of recovery annealing prior to solutionizing is optimized to release the stored energy gradually and, in the process, reduce or even eliminate the driving force for recrystallization. It shows that ramping the annealing temperature continuously and slowly is probably the most effective way to achieve it. Through this approach, a NBSC superalloy strained to 5.9% is successfully recovered, and recrystallization is fully preempted. In other words, the supersolvus critical strain has been pushed to 5.9%, which is about 3–5 times higher than those previously reported [10]. It must be emphasized here that in the plastically compressed cylinders, dislocation slip bands, around which the strains are concentrated locally, are readily observed at 45$^{\mathrm{o}}$ to the loading direction. Most of the plastic strains are accommodated in the slip bands, while the strains are much lower in regions that are outside of the bands. Therefore, the successfully recovered local plastic strains are likely to be far higher than the measured global strains.

In the deformed specimens, strain-induced misorientation within the non-recrystallized grains persists even after recovery annealing and solutionizing; such misorientation appears to increase with ϵ_p. Different from HAGBs that are rendered by recrystallization, the misorientation appears with a continuous orientation gradient without any abrupt change or sharp boundary. From Figure 1e, a misorientation of 13° over a length of 3 mm is found. As displayed in Figure S5, the density of the geometrically necessary dislocations required for it is estimated to be of order of 10^{12} m^{-2} [19], which is relatively low and consistent with the observation made on Figure 2b. Prolonging the solutionizing treatment does not appear to reduce the misorientation (Figure S6), suggesting that the remnant geometrically necessary dislocations are hard to eliminate through annealing. The prolonged solutionizing experiment also proves that the stored energy has been eliminated completely, and thus recrystallization will not be triggered with a longer annealing time.

The recovery annealing strategy developed in this study has been explored on another brand of room temperature deformed NBSC superalloy: SRR99. By applying the continuous ramp-up recovery protocol, the supersolvus critical plastic strain is measured to be no lower than 4.6% (Figure S7), confirming a wider applicability of such a heat treatment protocol. Successful recovery annealing at 1100 °C for 6 h has been reported recently to preempt recrystallization in the 3D-printed NBSC superalloys, which intrinsically contain high and nonuniformly distributed residual strains [11], as well as in the NBSC superalloys tensile crept to 0.15% plastic strain [20]. More systematic study is needed to confirm whether the recovery of the plastic strains can be accomplished in a significantly shorter period. This may be tedious because the recovery annealing time that is necessary is a function of the magnitude of pre-strain. Practically, a two-hour pre-solutionizing recovery annealing is completely acceptable from both the productivity and energy consumption perspectives, because it is a relatively short period compared to those of the industrial standard heat treatments, which usually contain several hours of supersolvus homogenization and then tens of hours aging annealing.

5. Conclusion

In summary, we demonstrate that Ni-based superalloy single-crystals can be successfully recovered without triggering recrystallization after being deformed plastically at room temperature in uniaxial compression by subjecting them to a sub-solvus annealing prior to the standard solutionizing heat treatment. Using a higher recovery annealing temperature favors the recovery of larger plastic strains. For reaching those and prevent any RX (during the subsequent solutionizing treatment), ramping the temperature slowly and continuously is optimal. With such a strategy, a maximum of 5.9% plastic strain is successfully recovered in AM3 superalloy single crystals, which is more than three times the plastic strains recovered (1–2%) in prior literature. During recovery, coarsening of the γ'-particles takes place along with partial dissolution, creating mobile γ/γ' interphase boundaries and more room for dislocations to be unpinned from the phase boundaries, interact to annihilate, and form the low-energy network configurations. Through such mechanisms, the total stored energy is effectively lowered. Thus, even after subsequent supersolvus solutionizing treatment, the single crystalline nature is maintained, and the dislocation density is brought down to the level comparable to that of the cast samples. Our investigation offers a practical way to protect the deformed single crystalline Ni-based superalloy parts from recrystallizing and sheds light on the lowering of the over-all cost of the turbine blades.

Disclosure statement

No potential conflict of interest was reported by the author(s).

Funding

This work was supported by National Science and Technology Major Project: [Grant Number 2019-VII-0019-0161]; National Natural Science Foundation of China: [Grant Number 51927801, U2032205, and 52271042]; Outstanding Young Scholar Program: [Grant Number 2020-JCJQ-009]; 111 Project 2.0: [Grant Number BP0618008]. We appreciate the support from the International Joint Laboratory for Micro/Nano Manufacturing and Measurement Technologies. We thank Instrumental Analysis Center of Xi'an Jiaotong University and Dr. Peng Zhang from CAMPNano for the assistance with TEM characterization, and Dr. Zhijun Li from Shanghai Institute of Applied Physics, Chinese Academy of Sciences for the EBSD analysis.

ORCID

Kai Chen http://orcid.org/0000-0002-4917-4445

References

[1] Pollock TM. Alloy design for aircraft engines. Nat Mater. 2016;15:809–815. doi:10.1038/nmat4709

[2] Bürgel R, Portella PD, Preuhs J. Recrystallization in single crystal of nickel base superalloy. In: Pollock TM, Kissinger RD, editor. superalloys 2000. Warrendale, PA: TMS; 2000. p. 229–238.

[3] Mathur HN, Panwisawas C, Jones CN, et al. Nucleation of recrystallisation in castings of single crystal Ni-based superalloys. Acta Mater. 2017;129:112–123. doi:10.1016/j.actamat.2017.02.058

[4] Panwisawas C, Mathur H, Gebelin JC, et al. Prediction of recrystallization in investment cast single-crystal superalloys. Acta Mater. 2013;61:51–66. doi:10.1016/j.actamat.2012.09.013

[5] Xie G, Wang L, Zhang J, et al. Orientational dependence of recrystallization in an Ni-base single-crystal superalloy. Scr Mater. 2012;66:378–381. doi:10.1016/j.scriptamat.2011.11.037

[6] Zambaldi C, Roters F, Raabe D, et al. Modeling and experiments on the indentation deformation and recrystallization of a single-crystal nickel-base superalloy. Mater Sci Eng A. 2007;454–455:433–440.

[7] Koff BL. Gas turbine technology evolution: A designer's perspective. J Propuls Power. 2004;20:577–595. doi:10.2514/1.4361

[8] Xie G, Zhang J, Lou LH. Effect of cyclic recovery heat treatment on surface recrystallization of a directionally solidified superalloy. Prog Nat Sci Mater Int. 2011;21:491–495. doi:10.1016/S1002-0071(12)60088-4

[9] Li Z, Xu Q, Xiong J, et al. Plastic deformation and recrystallization of a Ni-based single crystal superalloy. Mater Sci Forum. 2016;850:47–55. doi:10.4028/www.scientific.net/MSF.850.47

[10] Panwisawas C, Mathur H, Gebelin JC, et al. Prediction of plastic strain for recrystallisation during investment casting of single crystal superalloys. In: Huron E, Reed RC, Hardy M, editor. Superalloys 2012. Warrendale, PA: TMS; 2012. p. 547–556.

[11] Chen K, Huang R, Li Y, et al. Rafting-Enabled recovery avoids recrystallization in 3D-printing-repaired single-crystal superalloys. Adv Mater. 2020;32:1907164.

[12] Shi D, Sui T, Li Z, et al. An orientation-dependent creep life evaluation method for nickel-based single crystal superalloys. Chinese J Aeronaut. 2022;35:238–249. doi:10.1016/j.cja.2021.03.003

[13] Li Y, Wang L, Zhao S, et al. Creep anisotropy of a 3rd generation nickel-base single crystal superalloy in the vicinity of [001] orientation. Mater Sci Eng A. 2022;848:143479. doi:10.1016/j.msea.2022.143479

[14] Norfleet DM, Dimiduk DM, Polasik SJ, et al. Dislocation structures and their relationship to strength in deformed nickel microcrystals. Acta Mater. 2008;56:2988–3001. doi:10.1016/j.actamat.2008.02.046

[15] Nabarro FRN. Rafting in superalloys. Metall Mater Trans A Phys Metall Mater Sci. 1996;27:513–530. doi:10.1007/BF02648942

[16] Borouni A, Kermanpur A. Effect of Ta/W ratio on microstructural features and segregation patterns of the single crystal PWA1483 Ni-based superalloy. J Mater Eng Perform. 2020;29:7567–7586. doi:10.1007/s11665-020-05189-8

[17] Kontis P, Li Z, Collins DM, et al. The effect of chromium and cobalt segregation at dislocations on nickel-based superalloys. Scr Mater. 2018;145:76–80. doi:10.1016/j.scriptamat.2017.10.005

[18] Giraud R, Hervier Z, Cormier J, et al. Strain effect on the γ' dissolution at high temperatures of a nickel-based single crystal superalloy. Metall Mater Trans A Phys Metall Mater Sci. 2013;44:131–146. doi:10.1007/s11661-012-1397-9

[19] Pantleon W. Resolving the geometrically necessary dislocation content by conventional electron backscattering diffraction. Scr Mater. 2008;58:994–997. doi:10.1016/j.scriptamat.2008.01.050

[20] Lin S, Shen H, Zhou G, et al. A new rejuvenation heat treatment of crept Ni-based superalloy single crystals. IOP Conf Ser Mater Sci Eng. 2022;1249:012017.